



## Extraction and characterization of microcrystalline cellulose from *Apocynum venetum*

A F M Fahad Halim<sup>a</sup>

Received 4 February 2020; revised received and accepted 9 March 2021

In this work, cellulose microcrystal has been isolated from *Apocynum venetum* (AV) through acid hydrolysis. In addition, the properties of microcrystalline cellulose (MCC-N) extracted from AV are compared with those of commercially available microcrystalline cellulose (MCC-C). The characterizations of MCCs are studied by X-ray diffraction, Fourier transforms infrared spectroscopy, scanning electron microscopy, thermo gravimetric analyzer, and Zeta potential. As compared to MCC-C, MCC-N unveil more crystallinity percentage, fewer impurities, and comparable thermal stability without modifying the chemical composition of the sample. Besides, SEM images demonstrate rough surface and slight aggregation of extracted MCC from AV. Extracted MCC from AV can be possibly utilized as a reinforcement in green composites or hydrophilic micro composites as well as a source for AV fibre derived nanocellulose. Moreover, MCC-N can also be used in food, cosmetics, and medical industries.

**Keywords:** *Apocynum venetum*, Bast fibre, Degumming, Microcrystalline cellulose

### 1 Introduction

Throughout the latter few periods, cellulose has become reliable, most plentiful, economic, non-toxic, renewable bio-macromolecules in nature and extensively applied in miscellaneous fields. Extraction of cellulose can be easily done from most of the natural fibres. Due to its excellent mechanical strength and noble heat resistance property, it can be used for polymer matrixes as an outstanding bio-filler.

Finding new yields that produce both fibre and by-products with the advancement of suitable innovation, has become fundamental issues. *Apocynum venetum* (AV) can be considered as a C3 plant enduring bush, broadly dispersed in saline territories, desert meadows, and alluviums in the Mediterranean and Northwestern China. This species plays an important role in local sand fixation and soil and water conservation<sup>1, 2</sup>. Throughout the moderate areas of North America, Europe, and Asia, nine species of the genus AV are distributed. After harvesting, the stems are first scattered over on the ground to dry, afterwards the wood parts and bark are removed mechanically<sup>3</sup>. The impurities such as pectin, lignin, and wax must be removed to produce clean fibers<sup>4</sup>. Degumming methods are either chemical or bacterial. However, extraction and dyeing of AV fibres are more troublesome than that of cotton<sup>5</sup>. The dry stem of AV accounts for 10.2-17% of the fibre<sup>3, 6</sup>. AV contents

include (w / w): 9.06% of pectin, 12.09% of lignin, 45.75% of cellulose, 16.31% of hemicellulose, 2.58% of wax and 15.22% of water-soluble substances<sup>7</sup>. The amount of AV vegetation all over China, natural or artificial, is 1,330,000 ha<sup>8</sup>. In recent years, AV made fabrics have drawn strong interest to improve the clothing industry for providing wearing comfort and protecting health. The research results show that fabrics made from AV can emit far-infrared light of a wavelength of 8-15  $\mu\text{m}$ , which helps to keep AV underwear warm more efficiently. Besides, underwear made of AV also has strong characteristics to block the ultraviolet with a permeability of only 2%, protecting human body from the ultraviolet radiation<sup>9</sup>. In addition, restorative properties make AV progressively appealing as a customary Chinese herbal medicine<sup>10</sup>.

The extraction of MCC from natural fibre by different methods has been investigated. Using acid hydrolysis method with 2.5N HCl, extraction of MCC from oil palm empty fruit bunch pulp was stated by Haafiz *et al.*<sup>11</sup>. Furthermore, from the same fruit, MCC was also extracted by Xiang *et al.*<sup>12</sup>, using 0.7% (w/v) NaClO<sub>2</sub>, and after that treated with 17.5% (w/v) NaOH, followed by 55% (w/w) H<sub>2</sub>SO<sub>4</sub>. Besides, Kian *et al.*<sup>13</sup> have described the extraction of MCC from Roselle fibres by bleaching with 10% (w/v) NaClO, scoured with 8.0% (w/v) NaOH, and hydrolyzed with 2.5mol/L HCl. Moreover, the removal of MCC from jute fibre has been done by Islam *et al.*<sup>14</sup>, applying 65% (w/w) H<sub>2</sub>SO<sub>4</sub>. Additionally, Hou *et al.*<sup>15</sup> have carried out the

<sup>a</sup>E-mail: fahadrabbyzstu@yahoo.com

separation of MCC from waste cotton fabrics by applying catalytic hydrolysis of phosphotungstic acid. In order to produce MCC commercially from wood and cotton, weak mineral acids are used<sup>16</sup>.

In this study, attempts have been made to extract MCC from AV fibres through an acid hydrolysis process. Furthermore, comparison between the properties of extracted MCC-N with that of MCC-C are also conducted.

## 2 Materials and Methods

### 2.1 Materials

AV plant stems were collected from Xinjiang Province, P.R. China. Since the medullary tissue of AV cannot be utilized to acquire fibres, it is mechanically or physically separated from the phloem section. The fibres were washed properly to remove the dirt, dust, and further remains, which was later dried in an oven for 24 h at 60°C. The fibres obtained were used as raw materials. The chemicals utilized in this study were provided by Shanghai Macklin Biochemical Co. Ltd. Raw fibre of *Apocynum venetum* (Raw), *Apocynum venetum* microcrystalline cellulose (MCC-N) and commercial microcrystalline cellulose (MCC-C) were used.

### 2.2 Traditional Degumming Method

Figure 1 depicts the traditional degumming process. Sequential degumming process steps followed in this study are given below:

Mechanically stripped bast » pretreatment (sample 6g raw fibre) » fibre wash » first chemical treatment » fibre wash » second chemical treatment » fibre wash » beating » acid treatment [98% H<sub>2</sub>SO<sub>4</sub> (1 g/L), 24°C, M:L-1:15, time 2 min] » fibre wash » bleaching [2% H<sub>2</sub>O<sub>2</sub>, 0.1% Tween-80 surfactant, temperature 94°C, M:L-1:15, time 1h] » fibre wash » drying (dried in oven at 105°C for 4 h)<sup>17</sup>.

### 2.3 Microcrystalline Cellulose Extraction

In the first place 3g of samples were treated with 4.5 mol/L HCl at 75°C for 3.5h with magnetic stirring

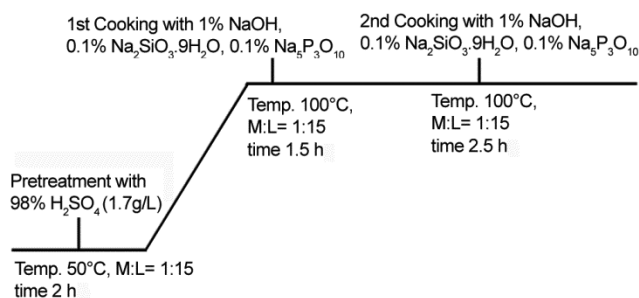


Fig. 1 — Traditional degumming process

having M: L ratio 1: 25. At the end, the suspension was diluted with cold distilled water. Subsequently, the suspension was filtered and washed repeatedly until the pH remains between 6 and 7. Afterwards, in a vacuum oven, the obtained MCC from AV was dried at 80°C for 5h.

### 2.4 Characterization

#### 2.4.1 X-ray Diffraction

The crystallization of the samples (Raw, MCC-N and MCC-C) was analyzed qualitatively by an ARL XTRA X-ray diffractometer. The scanning speed is kept 3°/min, 2 theta is 3° -50°, and the wave length of copper target diffraction is 0.155nm. The formula for the calculation of the crystallinity index (CI) is shown below<sup>18</sup>:

$$CI = (I_{002} - I_{am}) / I_{002} \times 100\% \quad \dots (1)$$

where  $I_{002}$  is the maximum intensity of the (002) lattice diffraction; and  $I_{am}$ , the intensity diffraction at  $2\theta=18^\circ$ . Crystalline and amorphous materials in cellulose are specified by intensity readings at peaks (002) and  $18^\circ$  respectively<sup>19, 20</sup>.

#### 2.4.2 FTIR Spectroscopy

A Fourier infrared spectrometer (Bruker Vertex 70) was used to determine the infrared spectrum of the sample, with a scanning speed of 10 kHz, a scanning interval of 2 cm<sup>-1</sup>, and a scanning range of 400-4000 cm<sup>-1</sup>.

#### 2.4.3 Thermal Analysis

A thermal analysis instrument (Q500 thermogravimetric analyzer) was used to determine the thermal stability of the samples. Firstly, 6 mg of sample was taken and then scanned at a heating rate of 20°C min<sup>-1</sup>, from 30°C to 900°C under a nitrogen gas atmosphere.

#### 2.4.4 Morphological Structure

In order to study the morphological characteristics, the Carl Zeiss SEM (model vltra55) was used. Before the observation, in order to avoid the charging effect, the sample was sputtered with gold.

#### 2.4.5 Zeta Potential Measurement

Using Zeta Meter ZM-77, electromotive force was evaluated by electrophoresis. Prior to testing, 5% (w / v) MCC-C and MCC-N solutions were prepared with distilled water and stirred for 5 min. Then diluted with distilled water at a ratio of 1:100 (v/v). Aliquots from the supernatant were used to measure zeta potential.

### 3 Results and Discussion

#### 3.1 FTIR Spectroscopy Study

Figure 2 displays the FTIR spectra of Raw, MCC-N, and MCC-C. It is clear from the spectral study that the absorption peak of  $3419\text{ cm}^{-1}$  for all samples is allocated to the OH group<sup>21, 22</sup>. Meanwhile, the absorption band at  $2919\text{ cm}^{-1}$  for the samples indicates CH and  $\text{CH}_2$  stretching vibrations<sup>22</sup>. Besides, absorption peaks at  $2357\text{ cm}^{-1}$  depict CH stretching of wax, which is completely eradicated from the samples MCC-N and MCC-C. Moreover, a vibrational peak is observed at  $1735\text{ cm}^{-1}$  in the spectrum of the Raw sample, which indicates the presence of C=O stretching of methyl ester and carboxylic acid or the acetyl group in hemicelluloses. In addition, no vibrational peak is observed at  $1735\text{ cm}^{-1}$  in the MCC-N and MCC-C samples, which indicates successful removal of the pectin and hemicelluloses during chemical treatment<sup>22</sup>. On the other hand, the absorption band at  $1629\text{ cm}^{-1}$  of the Raw sample attributed to antisymmetric COO<sup>-</sup> stretching is drastically decreased for MCC-N demonstrating the efficacy of the extraction method to remove lignin<sup>21</sup>. Besides, due to the cellulose structure absorption peaks at  $1157\text{ cm}^{-1}$  and  $1058\text{ cm}^{-1}$  in the fingerprint regions can be seen for all the samples<sup>21, 22</sup>. The wave number at  $895\text{ cm}^{-1}$  represents the  $\beta$ -1,4-glycoside bonds of cellulose<sup>23</sup>. From the spectral study of the samples, we can conclude that the main non-cellulosic constituents were removed from MCC-N by its respective chemical treatment, representing that the extraction process is satisfactory in comparison with MCC-C.

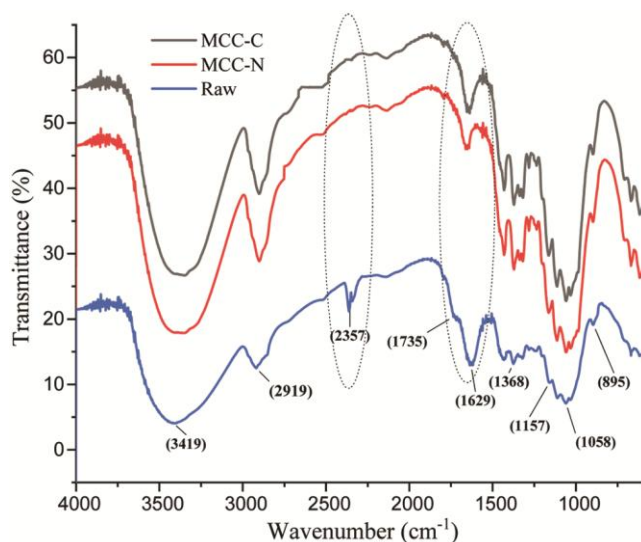


Fig. 2 — FTIR spectra of different samples

#### 3.2 X-ray Diffraction

In order to clearly understand the crystal structure of MCC extracted from AV, the samples are subjected to XRD testing. It can be clearly seen from Fig. 3 that the original sample shows that the cellulose I structure has diffraction peaks at  $15.2^\circ$ ,  $17.2^\circ$ ,  $21.2^\circ$ ,  $22.96^\circ$ , and  $34.5^\circ$ , which are respectively assigned to (101), (10 $\bar{1}$ ), (021), (002), and (040) planes<sup>24</sup>. This verifies that the application of acid hydrolysis has not changed the crystal structure of AV fibres. As compared to Raw, the diffraction peak intensities in samples MCC-C and MCC-N are stronger, indicating that the extracted AV MCC has an excellent crystal structure. Findings show that the crystallinity index (CI) is in the order: MCC-N (78.63%) > MCC-C (74.29%) > Raw (51.21%). The increase in CI is attributed to the amorphous region of cellulose dissolved in the fiber bundle after treatment with HCl, while adjusting its crystal structure and increasing the crystallinity of cellulose. CI increases with the transformation of micro to nano-fibrils<sup>25</sup>. Nevertheless due to acid hydrolysis, hydronium ions penetrate into the amorphous region of the cellulose, which stimulates the hydrolytic cleavage of glycosidic bonds and eventually releases distinct microcrystals<sup>26, 27</sup>. High

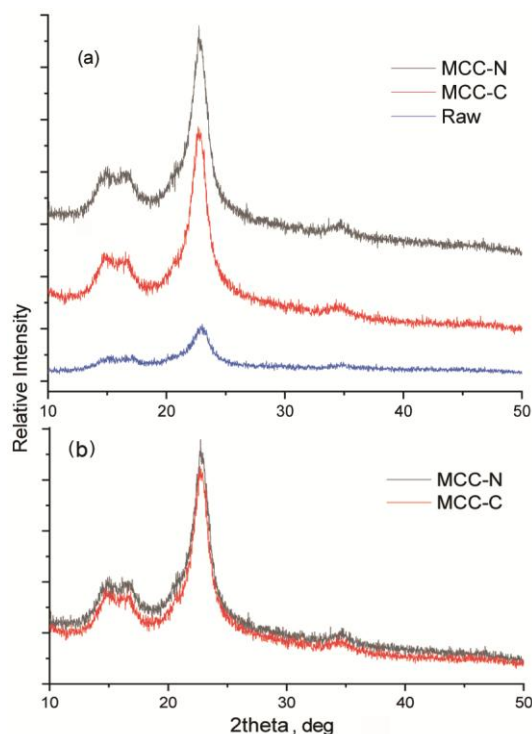


Fig. 3 — Diffraction patterns of (a) Raw and MCC-C, MCC-N at fixed intensity interval, and (b) MCC-N and MCC-C at the same intensity

crystallinity can achieve high strength, but instead it will show less hygroscopicity and reactivity with chemicals<sup>28</sup>. Furthermore, the higher CI of MCC-N than that of MCC-C represents that the extraction procedure is acceptable.

### 3.3 Morphological Structure

Figure 4 represents the Scanning electron micrographs of Raw, MCC-N and MCC-C. Like other bast fibres, AV fibres are bound by a protective layer composed of hemicellulose, lignin and pectin [Fig. 4(a)], which helps to protect AV from damage from the exterior environment. Figure 4(b) shows individualized fibres of AV. The reason for individualized fibers is due to the dissolution of

impurities, like pectin, lignin, wax, etc. during traditional degumming process which consists of acidic pretreatment and alkaline boiling<sup>17</sup>. In the meantime, the surface of degummed fibres is even and clean. Compared with Raw, MCC-N illustrates altered and non-uniform shapes with rougher surface. The reason behind this is that due to the HCl treatment, the fibre chain structure is degraded internally, resulting in the formation of small crystallites<sup>29,30</sup>. In addition, compared with MCC-C, MCC-N has less aggregate structure and narrower microstructure. This may be due to differences in cellulosic materials and separate chemical processing conditions<sup>31</sup>. MCC-N is suitable for the manufacture of high tensile strength

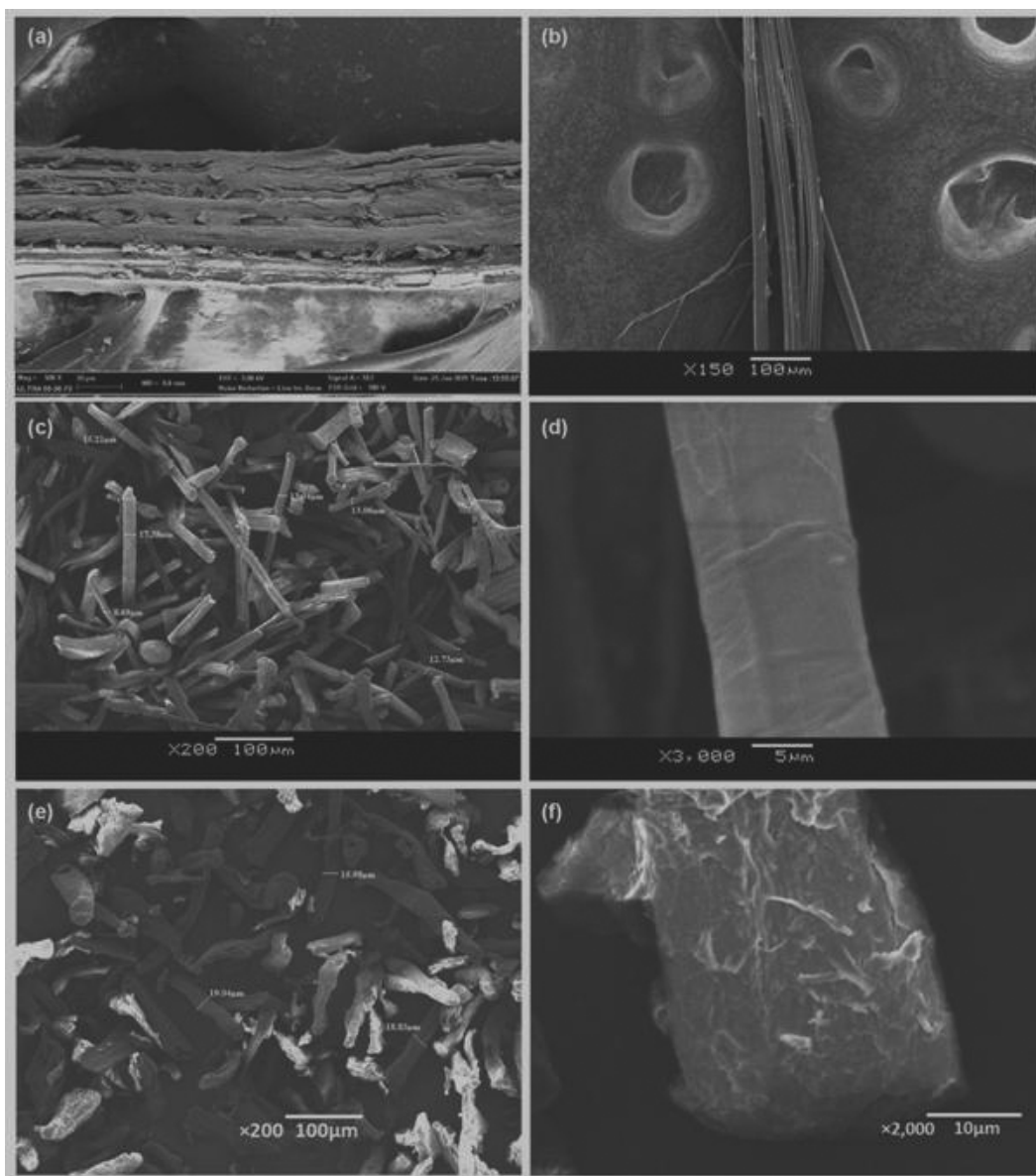


Fig. 4 — SEM images of (a) bast fibres, (b) traditional degummed fibres, (c) MCC-N, (d) single MCC-N, (e) MCC-C, and (f) single MCC-C

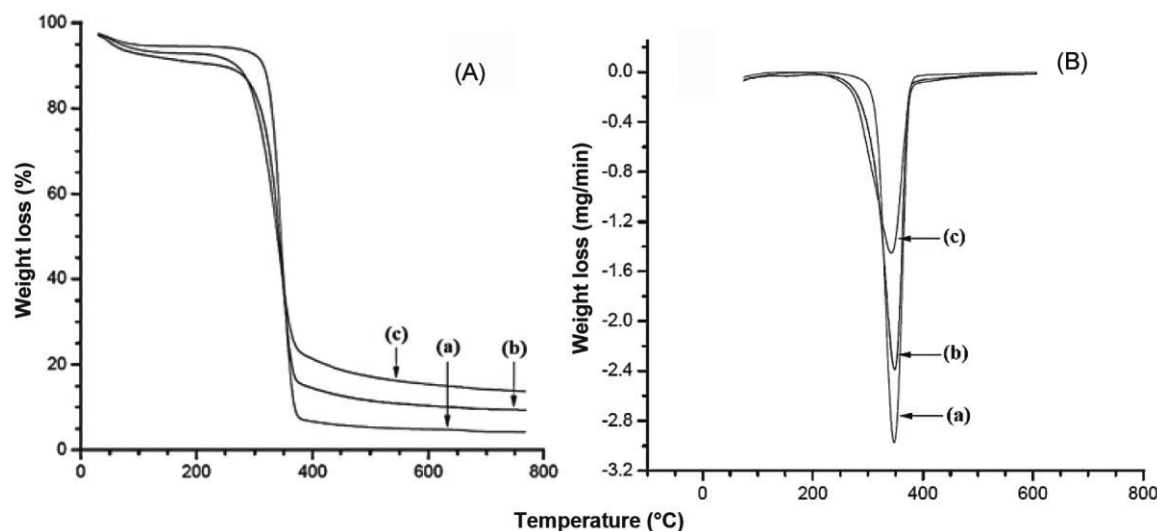


Fig. 5 — Showing (A) TGA and (B) DTG curves of (a) MCC-C, (b) MCC-N, and (c) Raw

bio-composite due to its long microfibrillar structure. Moreover, nanocrystals isolation can also be done from MCC-N.

### 3.4 Thermal Analysis

Figure 5 represents the thermogravimetric analysis curves of Raw, MCC-N, and MCC-C samples. It is evident from the curves that each sample depicts dual-phase thermal degradation outlines. Initial weight loss due to water vaporization and other unstable constituents in the sample takes place between the temperature range 60-150°C. Cellulose decomposition for Raw and MCC-N starts from 296.4°C and 313.9°C respectively. Instead, the temperature of degradation peak for Raw and MCC-N are 334.6°C and 339.4°C respectively. Cellulose degradation starts from 150°C and lasts up to 380°C and within this range depolymerization, decarboxylation, and decomposition occurs. Above 380°C, biomass undergoes aromatization, combustion, pyrolysis of lignin, and formation of residual carbon<sup>32-34</sup>. MCC-N show similar thermal constancy to MCC-C as far as initial deterioration and degradation peak temperature at 313.9 and 339.4°C, which may be influenced by dissimilar size of crystal<sup>35</sup>. Table 1 represents the TGA initial ( $T_{\text{initial}}$ ) temperature and DTG peak ( $T_{\text{peak}}$ ) temperature with char residue weight ( $W_{\text{residue}}$ ). Raw sample specify highest loss of weight at a lower temperature in comparison with MCC-N. The reason behind this is the high purity of cellulose in MCC-N<sup>36, 37</sup>. Compared with Raw, the weight of char residue for MCC-N is lower. Because of char formed from flame retardant constituents Raw samples shows high residual<sup>38, 39</sup>.

Table 1 — Thermal analysis data and Zeta potential of different samples

Samples	TGA and DTG analysis			Zeta potential, mV
	$T_{\text{initial}}, ^\circ\text{C}$	$T_{\text{peak}}, ^\circ\text{C}$	$W_{\text{residue}}, \%$	
Raw	296.4	334.6	12.34	
MCC-N	313.9	339.4	8.39	$-21.09 \pm 2.05$
MCC-C	325.3	343.8	3.58	$-30.72 \pm 3.06$

### 3.6 Dispersion Stability

The Zeta potential values of MCC-C and MCC-N are shown in Table 1. It is measured to analyze the dispersion stability of the extracted MCC's. It is known that when the value of Zeta potential is greater than 25 mV, the suspension is considered as stable. It can be concluded that MCC-N is more stable than MCC-C.

## 4 Conclusion

In this study, efforts have been made to extract MCC from AV by MCC-N process. FTIR spectra of MCC-N verifies that the application of acid has not changed the crystal structure of AV fibres. SEM micrographs show that MCC-N has a rougher structure and fewer large structure than MCC-C. Compared with MCC-C, MCC-N has a high crystallinity of 78.63%, which shows that it is suitable as a load-bearing material in composite structures. Besides, according to the values of zeta potential MCC-N is more stable than MCC-C. Furthermore, TGA analysis of MCC-N shows comparable thermal stability with MCC-C and thus it could be used for polymeric composites which could withstand high temperature. Another application could be extraction of nanocrystals and nanocomposites for various applications.

## References

- 1 Kim D-W, Yokozawa T, Hattori M, Kadota S & Namba T, *Ethnopharmacology*, 72 (2000) 53.
- 2 Xie W, Zhang X, Wang T & Hu J, *Ethnopharmacology*, 141 (2012) 1.
- 3 Berljand S, *Agro-Technology of Kendir* (NAUK, Moscow), 1950.
- 4 Wang L, Han G & Zhang Y, *Carbohydrate Polym*, 69 (2007) 391.
- 5 Liu Z & Zhou Y, *Plant Fibre Products*, 24 (2002) 30.
- 6 Weiming Z, Zhengchun X, Guanglun Z & Gongping G, *Chinese Wild Plant Resources*, 4 (2006).
- 7 Han, Ju, Liu & Zheng, *Proceeding of 83<sup>rd</sup> TIWC*, 1 (2004) 24.
- 8 TANG X, *Qinghai Agriculture*, 17 (2008) 48.
- 9 Häkkinen S & Auriola S, *Chromatography A*, 829 (1998) 91.
- 10 Cui Y-N, Xia Z-R, Ma Q, Wang W-Y, Chai W-W & Wang S-M, *Plant Physiology Biochem*, 135 (2019) 489.
- 11 Haafiz M M, Eichhorn S, Hassan A & Jawaid M, *Carbohydrate Polym*, 93 (2013) 628.
- 12 Xiang L Y, Mohammed M A P & Baharuddin A S, *Carbohydrate Polym*, 148 (2016) 11.
- 13 Kian L K, Jawaid M, Ariffin H & Alothman O Y, *Biological Macromol*, 103 (2017) 931.
- 14 Islam J M, Hossain M A, Alom F, Khan M I H & Khan M A, *Composite Materials*, 51 (2017) 31.
- 15 Hou W, Ling C, Shi S & Yan Z, *Biological Macromol*, 123 (2019) 363.
- 16 Chuayjuljit S, Su-uthai S & Charuchinda S, *Waste Management Res*, 28 (2010) 109.
- 17 ZHANG Y-m & HAN G-t, *China's Fiber Products*, 2 (2005).
- 18 Segal L, Creely J, Martin Jr A & Conrad C, *Text Res J*, 29 (1959) 786.
- 19 Ganjyal G, Reddy N, Yang Y & Hanna M, *Appl Polym Sci*, 93 (2004) 2627.
- 20 Weimick P H, LaForge J J & Jacobs R S, *Fall Technical Conference and Trade Fair, Tappi* (Atlanta, USA), 2002, 276.
- 21 Durig J R, Craven S & Harris W, *Vibrational Spectra and Structure* (Elsevier, Amsterdam), 1981.
- 22 Silverstein R M & Webster F X, *Spectrometric Identification of Organic Compounds*, 6th edn (Wiley, New York), 1998.
- 23 Fan M, Dai D & Huang B, *Fourier Transform-Materials Analysis* (Intechopen), 2012.
- 24 Pearce E M, *Handbook of Fiber Science and Technology: Fiber Chemistry*, Vol 4 (Marcel Dekker Incorporated), 1985.
- 25 Lee S-Y, Mohan D J, Kang I-A, Doh G-H, Lee S & Han S O, *Fiber Polym*, 76 (2009) 94.
- 26 de Souza Lima M M & Borsali R, *Macromolecular Rapid Communications*, 25 (2004) 771.
- 27 Reddy N & Yang Y, *Green Chem*, 7 (2005) 190.
- 28 Elanthikkal S, Gopalakrishnanpanicker U, Varghese S & Guthrie J T, *Carbohydrate Polym*, 80 (2010) 852.
- 29 Owolabi A F, Haafiz M M, Hossain M S, Hussin M H & Fazita M N, *Biological Macromol*, 95 (2017) 1228.
- 30 Adel A M, El-Wahab Z H A, Ibrahim A A & Al-Shemy M T, *Bioresource Technol*, 101 (2010) 4446.
- 31 Jahan M S, Saeed A, He Z & Ni Y, *Cellulose*, 18 (2011) 451.
- 32 Sonia A & Dasan K P, *Carbohydrate Polym*, 92 (2013) 668.
- 33 Jonoobi M, Khazaeian A, Tahir P M, Azry S S & Oksman K, *Cellulose*, 18 (2011) 1085.
- 34 Kim U-J, Eom S H & Wada M, *Polym Degradation Stability*, 95 (2010) 778.
- 35 Trache D, Donnot A, Khimeche K, Benelmir R & Brosse N, *Carbohydrate Polym*, 104 (2014) 223.
- 36 Hussin M H, Pohan N A, Garba Z N, Kassim M J, Rahim A A, Brosse N, Yemloul M, Fazita M N & Haafiz M M, *Biological Macromol*, 92 (2016) 11.
- 37 Razali N, Salit M S, Jawaid M, Ishak M R & Lazim Y, *BioResources*, 10 (2015) 1803.
- 38 Neto W P F, Silvério H A, Dantas N O & Pasquini D, *Industrial Crops Products*, 42 (2013) 480.